Mat. Res. Soc. Symp. Proc. Vol. 721 © 2002 Materials Research Society

Crystallographic and Magnetic Properties of CoCrPt Thin Films Investigated Using Single-Crystal Perpendicular Magnetic Thin Film Samples

Masaaki Futamoto, Kouta Terayama[1], Katsuaki Sato[1], Nobuyuki Inaba[2], and Yoshiyuki Hirayama
Central Research Laboratory, Hitachi Ltd. Kokubunji, Tokyo 185-8601, Japan
[1]Tokyo University of Agriculture and Technology, Koganei, Tokyo 184-8588, Japan
[2]Development and Technology Division, Hitachi Maxell Ltd., Tsukuba, Ibaraki, 300-2496

ABSTRACT

Conditions to prepare good single-crystal CoCrPt magnetic thin film with the easy magnetization axis perpendicular to the film plane were investigated using oxide single-crystal substrates, Al_2O_3(0001), $LaAlO_3$(0001), mica(0001), $SrTiO_3$(111), and MgO(111). The best CoCrPt(0001) single-crystal thin film was obtained on an Al_2O_3(0001) substrate employing a non-magnetic CoCrRu underlayer. The crystallographic quality of single-crystal thin film was investigated using X-ray diffraction and high-resolution transmission electron microscopy. Some intrinsic magnetic properties (Hk, Ku) were determined for the single-crystal $CoCr_xPt_y$ thin films for a compositional range of x=17 – 20at% and y=0 – 17at%.

INTRODUCTION

Co-based alloy thin films are used as magnetic recording media in hard disk drives. The areal density will continuously increase to 100 – 200 Gb/in^2 in the near future. Perpendicular magnetic recording is expected to replace longitudinal magnetic recording to keep the thermal stability of recorded information at high densities. Improvements of magnetic properties while enhancing thermal stability are important issues for designing perpendicular magnetic recording media. The thermal stability and recording characteristics of future recording media have been studied mainly by computer simulation employing basic magnetic properties of Co-alloy materials such as magneto-crystalline anisotropy energy (Ku), exchange stiffness constant, Curie temperature, etc. However it has not been easy to determine these intrinsic basic magnetic properties using a polycrystalline magnetic thin film which consists of very small crystalline grains with complicated microstructure. In order to investigate the basic magnetic properties accurately, it is desirable to use well-defined single-crystal thin films.

Single crystalline Co-based alloy thin films with the easy magnetization axis perpendicular to the film plane have been prepared using Ti and Ru underlayers on mica(0001) substrates [1,2], and using a Ti/Ag composite underlayer on Si(111) substrates [3]. However, the Co-based alloy single-crystalline thin films are reported to include some crystallographic defects such as sub-grain boundaries and a small fraction of *fcc* Co-alloy. We have recently found that Co-alloy single-crystal thin films with the c-axis

perpendicular to the film plane can be grown on oxide single-crystal substrates [4] and that the crystallographic quality depends strongly on the substrate and underlayer materials.

In the present work, effects of substrate and underlayer materials on the crystallographic quality of CoCrPt alloy magnetic thin films will be discussed based on the structural analysis using X-ray diffraction and transmission electron microscopy studies. Using the optimized condition in growing good single-crystal thin films, CoCrPt alloy thin films with different compositions are prepared to investigate the basic magnetic properties.

EXPERIMENTAL PROCEDURE

Single-crystal oxides of Al_2O_3(0001), $LaAlO_3$(0001), mica(0001), $SrTiO_3$(111), and MgO(111) were chosen as possible substrates to grow exitaxial CoCrPt magnetic thin films with the *hcp*-basal plane (0001) parallel to the substrate surface. These oxide single-crystals were selected by taking into account the arrangements of metallic atoms in the surface which may affect the epitaxial growth of metallic films with *hcp* structure. The lattice misfit of CoCrPt layer against substrate material was ranged from nearly zero (mica) to more than 10 % (MgO). A DC magnetron sputtering system with the base pressure below 1 x 10^{-10} Torr was used to prepare thin film samples [5]. The background pressure increased to about 1 x 10^{-9} Torr when the substrates were heated to 500 – 600 K using lamp heaters. Non-magnetic underlayer materials with *hcp* crystal structure, $TiCr_{10}$, $CoCr_{40}$, $CoCr_{25}Ru_{25}$, $CoCr_{25}Ru_{25}$/Ti, were employed. A non-magnetic underlayer and a $CoCr_{19}Pt_{10}$ magnetic layer were sequentially sputter-deposited on oxide single-crystal substrates kept at 533 K. Before sputter deposition, the substrates were kept on a heating stage in the deposition chamber for about an hour to remove the surface contamination and to saturate the substrate temperature. The deposition rates were 1.7 – 1.8 nm/s for the Co-alloy materials and 0.8 – 0.9 nm/s for the Ti and TiCr materials, respectively. The composition of $CoCr_xPt_y$ magnetic layer was also varied by changing the sputtering target composition in the range for y= 0 – 17 at% while trying to keep the Cr content to be constant at around x=18 at%. The $CoCr_xPt_y$ magnetic layer thickness was varied between 6 and 100 nm.

The sample structure was investigated by X-ray diffraction employing θ-2θ, rocking curve and pole-figure techniques. Cross-sectional and plan-view sample structures were observed by using a high-resolution transmission electron microscope (TEM). Microscopic compositional distributions of alloy elements were studied by TEM equipped with a chemical analysis facility. A focused electron beam of 2 nm in diameter was employed in the electron-probe micro analysis (EPMA) to determine the local compositional variations.

RESULTS AND DISCUSSION

Effect of substrate material

Table I summarizes the experimental results. Here a $CoCr_{25}Ru_{25}$(50 nm) non-magnetic underlayer and a $CoCr_{19}Pt_{10}$(25 nm) magnetic layer were sequentially deposited on various substrates in the sputter deposition system simultaneously. Single-crystal thin films were obtained on Al_2O_3(0001), $LaAlO_3$(0001), and $SrTiO_3$(111) substrates, while polycrystalline thin films grew on mica(0001), MgO(111), and glass substrates. The glass substrate was used as a reference. The result that a

Table I Lattice parameters of substrate materials and results of X-ray analysis on CoCrPt/CoCrRu bi-layers formed on various single-crystal oxides.

Material	Al_2O_3 (0001)	$LaAlO_3$ (0001)	Mica (0001)	$SrTiO_3$ (111)	MgO (111)	Glass (reference)
Crystal structure	hexagonal	hexagonal	hexagonal	cubic	cubic	(amorphous)
Lattice constant						
a (nm)	0.475	0.537	0.518	$\sqrt{2}$a=0.552	$\sqrt{2}$a=0.595	-
c (nm)	1.299	1.311	20.99	-	-	-
Mismatch[1] (%)	-6.1[2]	-3.9[3]	-0.4[3]	-6.5[4]	-13.3[4]	-
Results of X-ray analysis						
I_{0002} (cps)	99200	13200	7400	8300	4600	1900
$\Delta\theta_{50}$ (degs)	0.6	2.6	5.3	5.1	6.3	7.6
Film quality	single-crystal	single-crystal	poly-crystal	single-crystal	poly-crystal	poly-crystal

Sample structure: CoCrPt(25nm)/CoCrRu(50nm)/Oxide single-crystal substrate.

1) Mismatch is calculated for the lattice parameter of $CoCr_{25}Ru_{25}$ non-magnetic underlayer, 2a=2x0.258 nm.
2) Al_2O_3(0001)//CoCr-alloy(0001), Al_2O_3[10.0]//CoCr-alloy[21.0]
3) $LaAlO_3$(0001) and mica(0001)//CoCr-alloy(0001), $LaAlO_3$[10.0] and mica[10.0]//CoCr-alloy[10.0].
4) $SrTiO_3$(111) and MgO(111)//CoCr-alloy(0001), $SrTiO_3[1\bar{1}0]$ and $MgO[1\bar{1}0]$//CoCr-alloy[10.0].

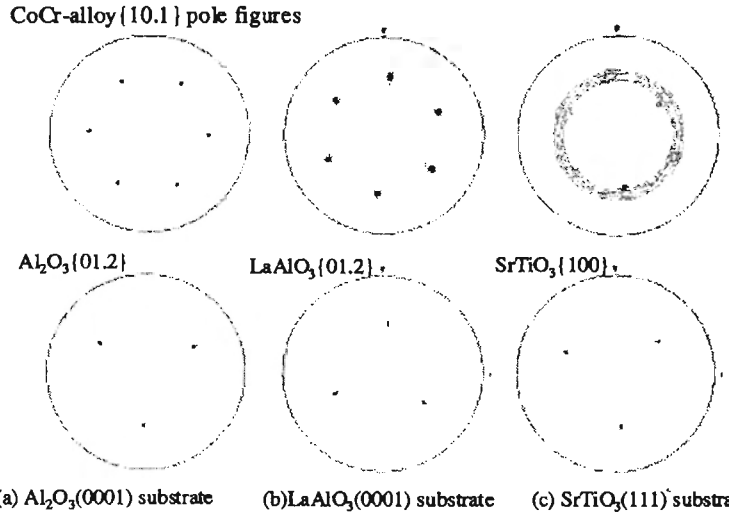

Figure 1 X-ray pole figure profiles of CoCrPt/CoCrRu layer and oxide single-crystal substrates.

polycrystalline CoCrPt magnetic thin film was obtained on the mica(0001) substrate, was against our expectation, since the lattice mismatch was the minimum among the film/substrate combinations investigated here. The mismatch is calculated using the lattice parameter values of substrate and underlayer materials. Single-crystal thin films could not be obtained on the mica(0001) substrate even when the CoCrPt magnetic thin film was deposited directly and with either a $TiCr_{10}$ or a $CoCr_{40}$ non-magnetic underlayer. Although the reason why single-crystal thin films could not be obtained on the mica(0001) substrates is unclear, the possibility to grow CoCrPt single-crystal thin films on mica remains high if an optimum film growth condition can be found.

Figure 1 shows the X-ray pole figures of Co-alloy{10.1} and those observed for the Al_2O_3{01.2}, $LaAlO_3${01.2}, and $SrTiO_3${100} planes. Epitaxial growth of CoCr-alloy thin film was confirmed on these oxide single-crystal substrates. Here the {10.1} reflections from the $CoCr_{19}Pt_{10}$ film and $CoCr_{25}Ru_{25}$ underlayer are overlapped because of a small difference in the lattice parameter ($CoCr_{19}Pt_{10}$: a=0.256 nm, $CoCr_{25}Ru_{25}$: a=0.258 nm). The pole figures of Co-alloy{10.1} planes show clear six-fold symmetry. This result indicates that the Co-alloy films are single-crystalline and possess specific crystallographic orientation relationships with the respective single-crystal substrates. The crystallographic relationships between Co-alloy thin film and substrate are determined to be Co-alloy(0001)[21.0]//Al_2O_3(0001)[10.0] on Al_2O_3(0001) substrate, Co-alloy(0001)[10.0]//$LaAlO_3$(0001)[10.0] on $LaAlO_3$(0001) substrate, and Co-alloy(0001)[10.0]//$SrTiO_3$(111)[1-10] on $SrTiO_3$(111) substrate, respectively.

The sharpness of {10.1} pole reflections is related to the crystallographic quality of the Co-alloy thin film. The Co-alloy thin film grown on the Al_2O_3(0001) substrate shows the $\Delta\theta_{50}$ value of 0.6 degree and very sharp {10.1} pole reflections, while the thin film on the $SrTiO_3$(111) substrate shows the $\Delta\theta_{50}$ value of 5.1 degrees and {10.1} pole reflections with large dispersions. The $CoCr_{19}Pt_{10}$ magnetic single-crystal thin film grown on the $SrTiO_3$(111) substrate is supposed to include crystallographic defects such as sub-grain boundaries noted in the previous works [1,3].

Effect of underlayer material

It is shown that a good single-crystal $CoCr_{19}Pt_{10}$ magnetic thin film can be grown on the Al_2O_3(0001) substrate. Then the effect of underlayer on the crystallographic quality of $CoCr_{19}Pt_{10}$ thin film was investigated using the Al_2O_3(0001) substrate. Table II compares the $\Delta\theta_{50}$ value, $\Delta\alpha_{50}$ value, and the quality of $CoCr_{19}Pt_{10}$ magnetic thin film when deposited via non-magnetic *hcp* underlayers. The $CoCr_{19}Pt_{10}$ magnetic thin film was also deposited directly on the Al_2O_3(0001) substrate. The $\Delta\alpha_{50}$ value is the FWHM of α-scan around the CoCrPt(10.1) pole in the X-ray pole figure measurement carried out to estimate the dispersion. A small $\Delta\alpha_{50}$ value corresponds to small (10.1) pole dispersion. Figure 2 shows the X-ray pole figure profiles of non-magnetic underlayer (Ti, $TiCr_{10}$) and Co-alloy layers. It is clear that the $CoCr_{19}Pt_{10}$ magnetic thin film quality depends strongly on the underlayer material. The

Table II Effect of underlayer material on $\Delta\theta_{50}$ and $\Delta\alpha_{50}$ values of Co-alloy film grown on Al_2O_3(0001) substrate

Underlayer	(no underlayer)	$TiCr_{10}$(30nm)	$CoCr_{40}$ (50nm)	$CoCr_{25}Ru_{25}$(50nm)	$CoCr_{25}Ru_{25}$(10nm)/Ti(50nm)
$\Delta\theta_{50}$ (degs)	3.5	3.0	2.2	0.6	0.9
$\Delta\alpha_{50}$ (degs)	4.0	5.1	3.3	1.8	2.3
Film quality	single-crystal	poly-crystal	poly-crystal	single-crystal	single-crystal

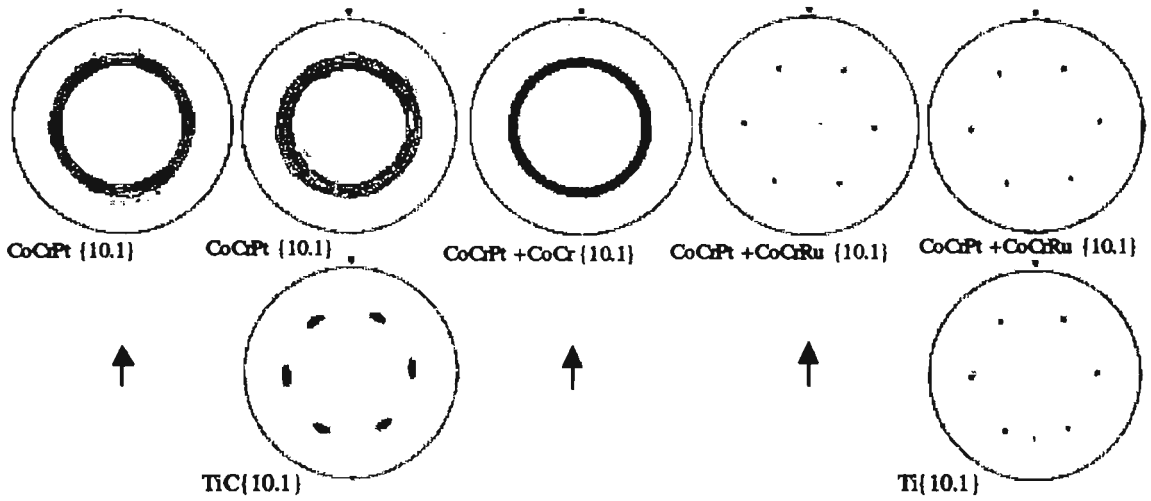

Figure 2 X - ray pole figure profiles of non-magnetic underlayer (Ti, TiCr) and CoCr-alloy layer. {10.1} poles of CoCrPt, CoCr, and CoCrRu are overlapped due to similar lattice constants.

best single-crystal $CoCr_{19}Pt_{10}$ magnetic thin film is obtained when deposited via a non-magnetic $CoCr_{25}Ru_{25}$ underlayer. Although a single-crystalline $CoCr_{19}Pt_{10}$ magnetic thin film can be obtained on the Al_2O_3(0001) substrate without any underlayer, the film quality is poor judging from the large values of $\Delta\theta_{50}$(3.5 deg.) and $\Delta\alpha_{50}$(4.0 deg.). The small mismatch in the lattice constant between the substrate and the deposited material does not explain the results shown in table II and figure 2. The $CoCr_{19}Pt_{10}$/ $CoCr_{25}Ru_{25}$ layer is a good single-crystal, while the $CoCr_{19}Pt_{10}$/$CoCr_{40}$ layer is polycrystalline where the misfits against the Al_2O_3(0001) substrate are similar for the respective underlayers ($CoCr_{25}Ru_{25}$: -6.12%, $CoCr_{40}$: -6.10%). It is also notable in figure 2 that the {10.1} poles from Ti underlayer (mismatch: 7.3%) show narrower distribution than that from the $TiCr_{10}$ underlayer with a little better mismatch of 7.1%. It seems necessary to take into account the other factor such as diffusion behavior of deposited materials on the substrate in the early stage of film growth to explain the results. An underlayer material that includes larger amount of Cr tends to show poor crystallographic quality. One possibility is that Cr element seems to suppress heteroepitaxial growth of deposited layer by suppressing the surface diffusion through combining selectively with oxygen atoms on the substrate surface. Addition of Ru to CoCr-alloy is considered to enhance surface diffusion when deposited on the Al_2O_3(0001) substrate. Further studies are necessary to make clear this interpretation.

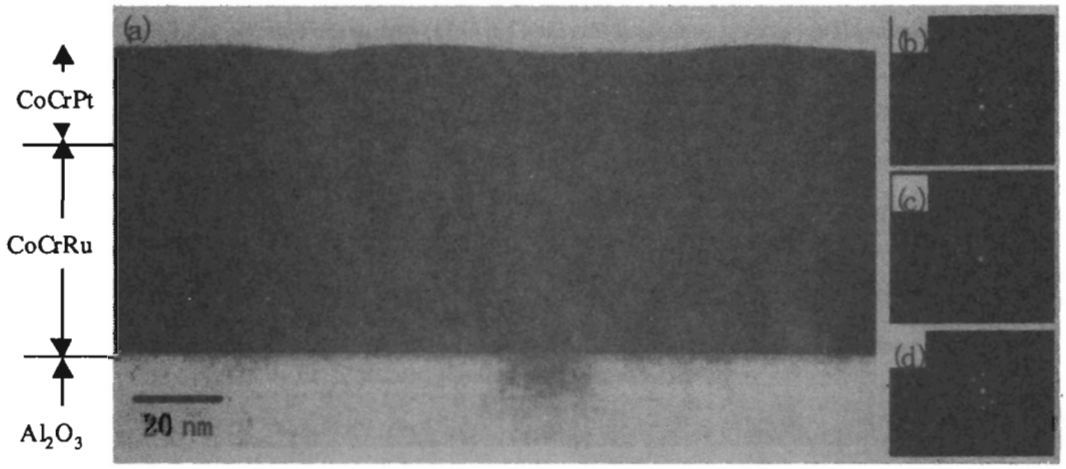

Figure 3 Cross-sectional structure and electron diffraction patterns of CoCrPt/CoCrRu/Al_2O_3 sample. (a) Cross-sectional structure. Electron diffraction patterns of (b), (c), and (d) were observed from CoCrPt, CoCrRu, and Al_2O_3 regions, respectively.

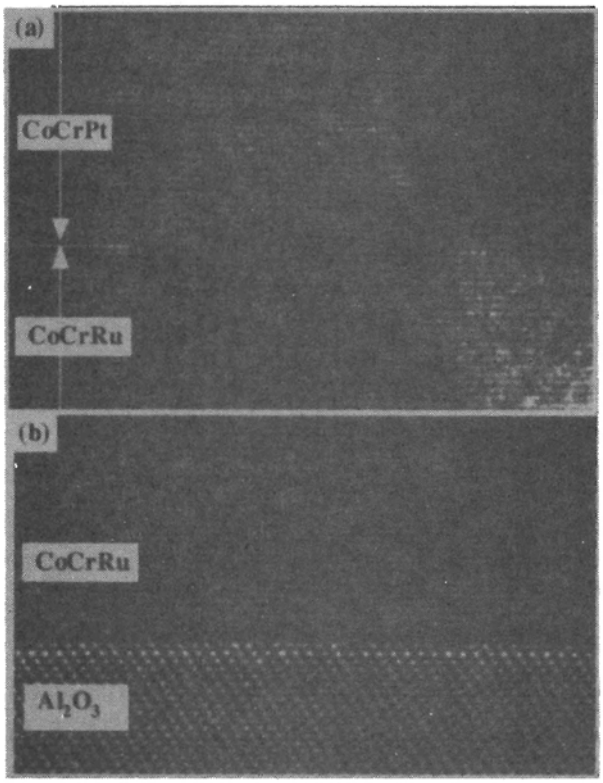

Figure 4 High-magnification TEM images of interfaces.
(a) Interface between CoCrPt and CoCrRu underlayer.
(b) Interface between CoCrRu underlayer and Al_2O_3 substrate.

Figure 3 shows the cross-sectional structure of a $CoCr_{19}Pt_{10}$(25 nm)/ $CoCr_{25}Ru_{25}$(50 nm)/ Al_2O_3(0001)

sample studied using a transmission electron microscope. There are no crystalline grain boundaries. In accordance with the X-ray pole figure results, a series of TEM diffraction patterns observed from the $CoCr_{19}Pt_{10}$ layer, the $CoCr_{25}Ru_{25}$ underlayer, and the $Al_2O_3(0001)$ substrate clearly indicates that the $CoCr_{19}Pt_{10}/CoCr_{25}Ru_{25}$ bi-layer is grown epitaxially on the $Al_2O_3(0001)$ substrate.

Figure 4 shows high-magnification TEM images observed around the interfaces of $CoCr_{19}Pt_{10}/CoCr_{25}Ru_{25}$ and $CoCr_{25}Ru_{25}/Al_2O_3(0001)$. Perfect hetero-epitaxy is realized between the $CoCr_{25}Ru_{25}$ nonmagnetic underlayer and the $CoCr_{19}Pt_{10}$ magnetic layer with no crystallographic defects around the interface.

Plan-view TEM structure of the $CoCr_{19}Pt_{10}$ magnetic layer is shown in figure 5. The sharp electron diffraction pattern and the high-resolution TEM picture clearly indicate that this film is a good quality single-crystal thin film and it has the easy magnetization axis (c-axis) perpendicular to the film plane.

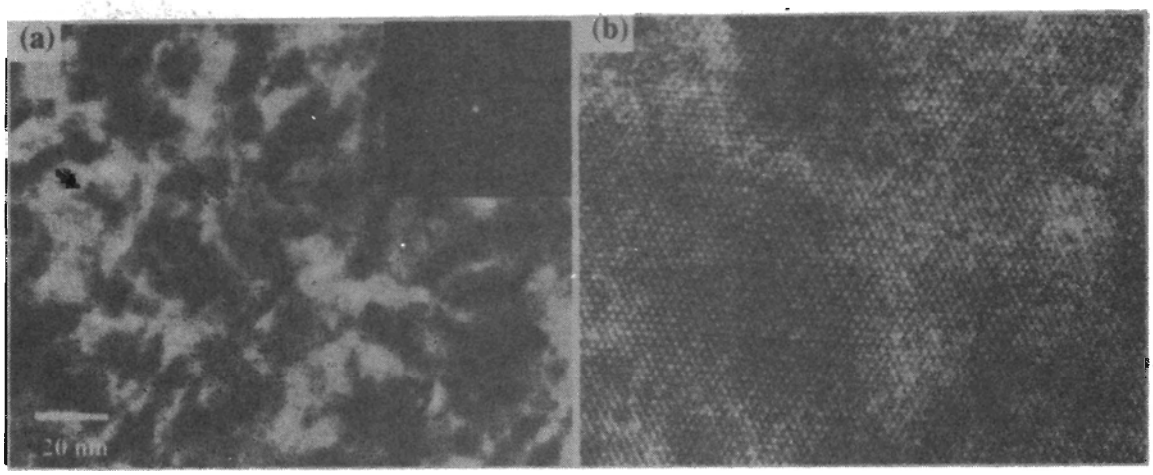

Figure 5 Plan-view TEM micrographs of single-crystal $CoCr_{19}Pt_{10}$ magnetic thin film grown on $Al_2O_3(0001)$ substrate. (a) Low magnification image and electron diffraction pattern. (b) High magnification lattice image.

Preparation of $CoCr_xPt_y$ single-crystal thin films

$CoCr_xPt_y$ single-crystal magnetic thin films were prepared employing the combination of $CoCr_{25}Ru_{25}$ underlayer (50 nm thickness) and $Al_2O_3(0001)$ single-crystal substrates. With this underlayer and substrate combination, it has been made clear that CoCrPt magnetic thin films with good crystallographic quality can be prepared. Here, we prepared $CoCr_xPt_y$ single-crystal thin films by changing the Pt content to investigate the effect of Pt concentration on basic magnetic properties. The Cr content in the magnetic thin film is tried to keep constant at around 18 at%. Table III summarizes the average film composition, lattice parameter, lattice mismatch between magnetic layer and underlayer, local composition, and Ku value of $CoCr_xPt_y$ single-crystal magnetic thin film. The thickness of magnetic layer was 50 nm. The average film composition was determined using Induction Coupled Plasma Spectroscopy (ICPS) and the local composition was investigated by using an EDAX-TEM. It is necessary to investigate the local distribution of alloy elements for these single-crystal magnetic thin

Table III Structural and magnetic properties of single-crystal CoCr-alloy thin films

Magnetic layer	Lattice parameter			Mismatch[1]	Local composition (at%)[2]			Ku (280 K)
	a (nm)	c (nm)	c/a	(%)	Co	Cr	Pt	x 10^6 erg/cm^3
$CoCr_{20}$	0.253	0.406	1.605	-1.98	80.4 (0.66)	19.6 (0.66)	-	1.6
$CoCr_{18}Pt_7$	0.255	0.410	1.606	-1.09	75.4 (1.04)	17.2 (1.12)	7.4 (0.61)	2.4
$CoCr_{19}Pt_{10}$	0.256	0.413	1.610	-0.66	71.2 (1.45)	17.9 (1.47)	10.9 (0.59)	3.0
$CoCr_{17}Pt_{17}$	0.258	0.416	1.613	-0.04	67.0 (0.96)	17.0 (0.80)	16.0 (0.67)	4.2
$(CoCr_{25}Ru_{25})$	0.258	0.411	1.593	-	-	-	-	-

Sample structure: CoCr-alloy thin film (50nm)/$CoCr_{25}Ru_{25}$(50nm)/Al_2O_3(0001).
1) Mismatch of *a* parameter between CoCr-alloy magnetic layer and CoCrRu underlayer.
2) Average local compositions are estimated from 24 spots analysis using EDAX-TEM.
Values in parenthesis are standard deviations (σ) of local fluctuation around the average compositions of Co, Cr, and Pt.

films, since a compositional inhomogeneity will change the local magnetic properties. Local fluctuations in alloy elements are expected because the Cr content in $CoCr_xPt_y$ layer is exceeding the solubility limit in the phase diagram of Co-Cr alloy system. The excess Cr and possibly also Pt atoms may localize even in the single-crystal thin films under the influences of various origins including stress, strain, crystallographic defects, etc.

Figures 6 and 7 show the local compositional distributions measured for the single-crystal thin films of $CoCr_{40}$ and $CoCr_{17}Pt_{17}$, respectively. The electron beam diameter in the EDAX-TEM analysis was 2 nm. The local compositions were measured along the A – B and the C – D lines as indicated in the plan-view TEM pictures. Slight compositional variations of Co and Cr elements are recognizable around the average values of Co (80.4%) and Cr (19.6%) in the $CoCr_{20}$ single-crystal thin film. No apparent relation between the compositional fluctuation and the TEM contrast is observed. The compositional fluctuation with wavelength of 30 – 40 nm is noted in figure 6. Similar compositional fluctuations are recognized for the $CoCr_{17}Pt_{17}$ single-crystal thin film as shown in figure 7. The Pt distribution seems to be almost independent to those of other elements, while Cr shows an opposite distribution profile to that of Co. The Cr element fluctuation around the average composition (17.0 at%) of the $CoCr_{17}Pt_{17}$ single-crystal thin film is $\pm$ 1.6% (2σ). The value is smaller than those observed for polycrystalline CoCr-alloy perpendicular recording media with similar Cr concentrations [6,7]. Local compositional analyses on $CoCr_{18}Pt_7$ and $CoCr_{19}Pt_{10}$ single-crystal thin films showed results similar to those of $CoCr_{20}$ and $CoCr_{17}Pt_{17}$ thin films depicted in figures 6 and 7.

The compositional fluctuation of Cr element is confirmed to be within $\pm$3 at% (2σ) for these single-crystal thin film samples. Pt element showed smaller fluctuations than that of Cr for all the samples as shown in the standard deviation values (α) listed in table III. A series of structural and compositional investigation has shown that the CoCr(Pt)-alloy thin films are single-crystals grown epitaxially on the Al_2O_3(0001) substrates and that these single-crystal thin films have compositional fluctuations of alloy elements to be within a few atomic percent around the average compositions.

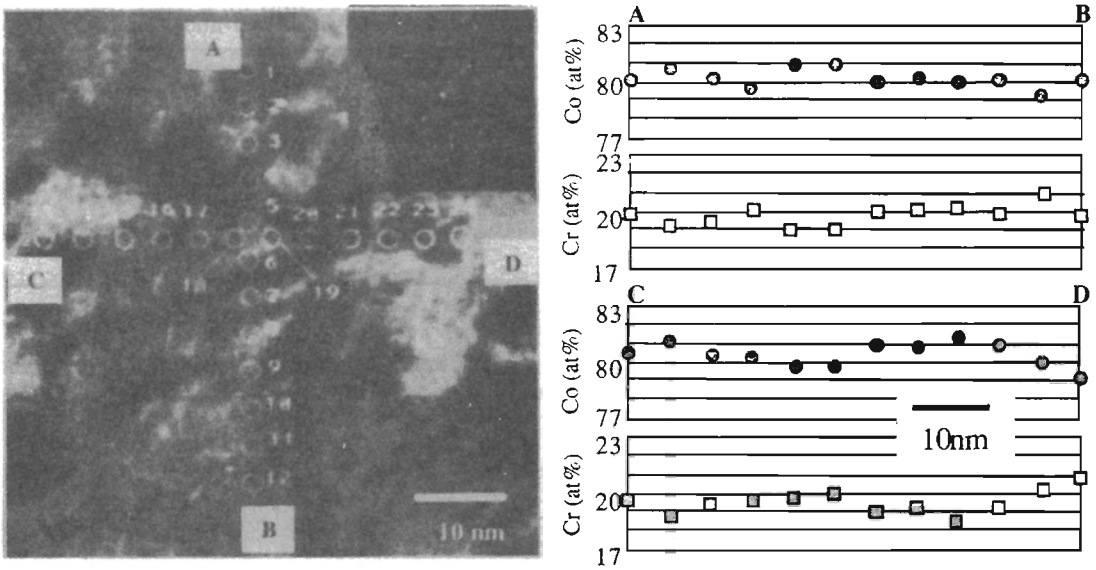

Figure 6 Local distributions of alloy elements measured for single-crystal $CoCr_{20}$ magnetic thin film. Local compositions were measured for analysis points along A - B and C - D lines shown in plan-view TEM picture.

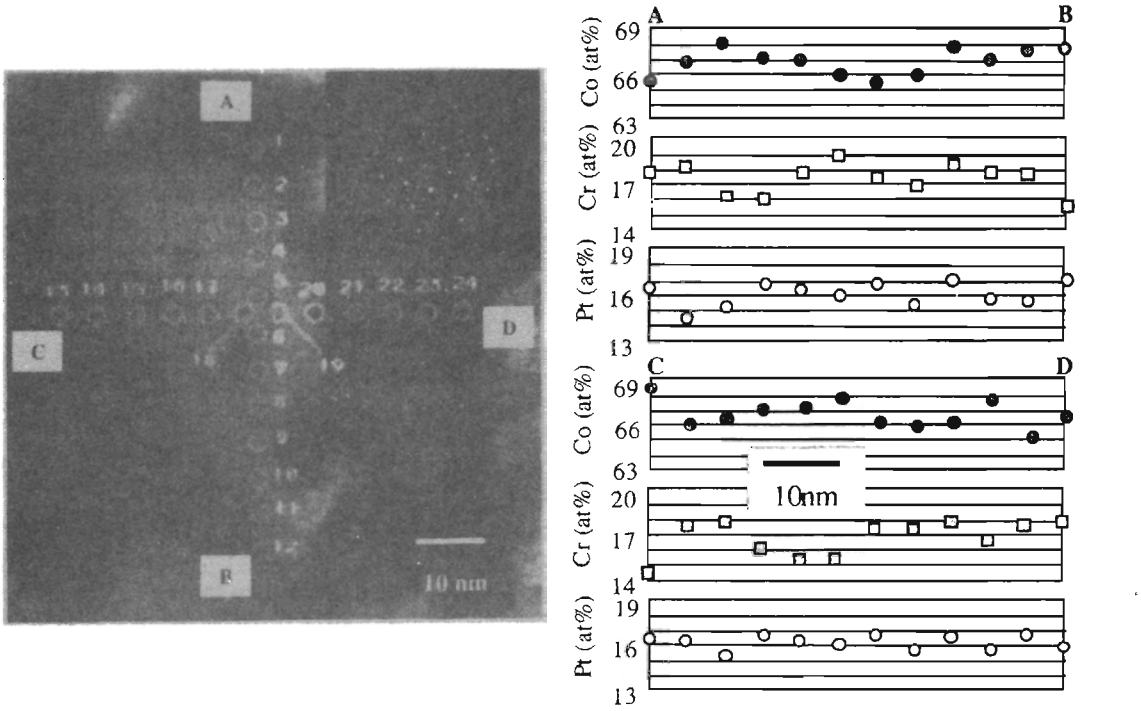

Figure 7 Local distributions of alloy elements measured for single-crystal $CoCr_{17}Pt_{17}$ magnetic thin film. Local compositions were measured for analysis points along A - B and C - D lines shown in plan-view TEM picture.

Magnetic properties of CoCrPt single-crystal thin films

Figure 8 shows the relationships between magnetic layer thickness and magnetic properties investigated using $CoCr_xPt_y$ single-crystal thin films. Ku value increases with increasing the Pt concentration. The Ku values of $CoCr_{20}$, $CoCr_{18}Pt_7$, $CoCr_{19}Pt_{10}$, and $CoCr_{17}Pt_{17}$ single-crystal thin films (50 nm thickness) are respectively determined to be 1.6, 2.4, 3.0, and 4.2 x 10^6 erg/cc at 280 K. It is noted that Hk and Ku values tend to decrease with decreasing the magnetic layer thickness for all the compositions. This decreasing tendency is clear especially for the reduced magnetic layer thickness below around 25 nm. Possible reasons for the decease in Hk and Ku are variations of local composition and crystallographic defect density close to the interface and/or the surface. Slight increase of Cr content close to the interface and/or the surface will reduce the local Hk and Ku values. Ku value decreases with increasing number of stacking faults. Stacking faults are reported to exist preferentially close to the underlayer in CoCrPt perpendicular recording media [8]. Single-crystal magnetic thin films will be studied to clarify for this preference.

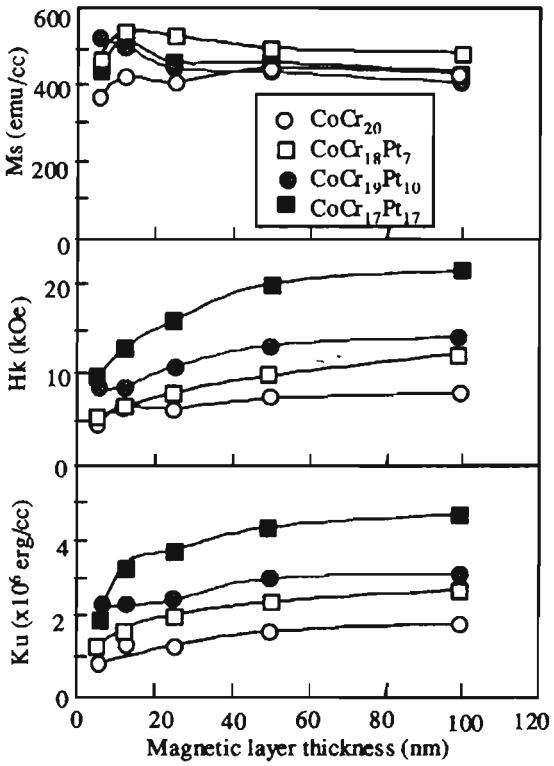

Figure 8 Magnetic properties of $CoCr_xPt_y$ single-crystal thin films investigated as a function of layer thickness.

Single-crystal magnetic thin films are useful to accurately determine the intrinsic magnetic properties. They are also useful for finding methods to improve the magnetic properties as the magnetic layer thickness becomes thinner than 20 – 30 nm level. This seems to be an inevitable path for designing future perpendicular recording media.

CONCLUSIONS

Conditions to prepare good single-crystal CoCrPt magnetic thin films are investigated using oxide single crystal substrates. Some intrinsic magnetic properties are determined as functions of composition and thickness for the CoCrPt single-crystal magnetic thin films. The following results are obtained.

(1) Single-crystal CoCrPt magnetic thin films with the c-axis perpendicular to the film plane can be grown on Al_2O_3(0001), $LaAlO_3$(0001), and $SrTiO_3$(111) substrates. The best CoCrPt(0001) single

crystal thin film with good crystallographic quality is obtainable on an Al_2O_3(0001) substrate employing a suitable non-magnetic underlayer with an *hcp* structure.

(2) The crystallographic quality of CoCrPt magnetic thin film strongly depends on the underlayer material. A high quality CoCrPt magnetic thin film is prepared when deposited on an Al_2O_3(0001) substrate via a CoCrRu non-magnetic underlayer.

(3) Compositional fluctuations of alloy elements (Cr, Pt) are observed for single-crystal $CoCr_xPt_y$ (0001) magnetic thin films (x=17 - 20at%, y=0 – 17at%). The fluctuations are confirmed to be less than ± 3 atomic percent (2σ) around the average compositions.

(4) Magnetic properties (Hk, Ku) are determined for the single-crystal $CoCr_xPt_y$ magnetic thin films with different Pt concentrations. The Ku value tends to decrease when the magnetic layer thickness becomes smaller than about 25 nm where the influence from the interface and the surface of the magnetic layer becomes prominent.

ACKNOWLEDGMENT

A part of this work was carried out under the ASET program supported by NEDO.

REFERENCES

1. K. M. Krishnan, Y. Honda, Y. Hirayama, and M. Futamoto, Appl. Phys. Lett. **64**, 1499-1501(1994).
2. K. M. Krishnan, T. Takeuchi, Y. Hirayama, and M. Futamoto, IEEE Trans. Magn. **30**, 5115-5119 (1994).
3. H. Hong, M. Rao, D. E. Laughlin, and D. N. Lambeth, J. Appl. Phys. **85**, 4699-4701 (1999).
4. K. Terayama, K. Sato, Y. Hirayama, N. Inaba, and M. Futamoto, J. Mag. Soc. Jpn. **Vol. 25**, 559-562 (2001) (in Japanese).
5. Y. Matsuda, M. Suzuki, Y. Hirayama, Y. Honda, and M. Futamoto, J. Mag. Soc. Jpn. **Vol.18**, Suppl. No.S1, 99-102(1994).
6. Y. Hirayama, M. Futamoto, K. Kimoto, and K. Usami, IEEE Trans. Magn. 32, 3807-3809 (1996).
7. M. Futamoto, N. Inaba, Y. Hirayama, K. Ito, and Y. Honda, Mat. Res. Soc. Symp. Proc. **Vol.517**, 243-254 (1998).
8. Y. Takahashi, K. Tanahashi, and Y. Hosoe, J. Appl. Phys. **91** (2002) (in press).